Medical Engineering & Physics 35 (2013) 88–95

Contents lists available at SciVerse ScienceDirect

Medical Engineering & Physics

journal homepage: www.elsevier.com/locate/medengphy

Application of near infrared (NIR) spectroscopy for determining the thickness of articular cartilage

I. Afara, S. Singh, A. Oloyede*

School of Engineering Systems, Institute of Health and Biomedical Innovation, Faculty of Built Environment, Queensland University of Technology, Brisbane, Australia

ARTICLE INFO

Article history:
Received 7 September 2011
Received in revised form 10 January 2012
Accepted 7 April 2012

Keywords:
Cartilage thickness
Near infrared (NIR) spectroscopy
Partial least squares (PLS)
Calibration
Prediction

ABSTRACT

The determination of the characteristics of articular cartilage such as thickness, stiffness and swelling, especially in the form that can facilitate real-time decisions and diagnostics is still a matter for research and development. This paper correlates near infrared spectroscopy with mechanically measured cartilage thickness to establish a fast, non-destructive, repeatable and precise protocol for determining this tissue property. Statistical correlation was conducted between the thickness of bovine cartilage specimens ($n = 97$) and regions of their near infrared spectra. Nine regions were established along the full absorption spectrum of each sample and were correlated with the thickness using partial least squares (PLS) regression multivariate analysis. The coefficient of determination (R^2) varied between 53 and 93%, with the most predictive region ($R^2 = 93.1\%$, $p < 0.0001$) for cartilage thickness lying in the region (wavenumber) 5350–8850 cm^{-1}. Our results demonstrate that the thickness of articular cartilage can be measured spectroscopically using NIR light. This protocol is potentially beneficial to clinical practice and surgical procedures in the treatment of joint disease such as osteoarthritis.

1. Introduction

The structural characteristics of articular cartilage play a significant role in determining its response to load and hence physiological functions. These properties include the entrapment architecture of its collagen–proteoglycan network, fluid component and osmotic pressure, and intrinsic stiffness. In its unloaded state, these elements combine to determine the characteristic thickness of the tissue's matrix. Loss of matrix, and hence thickness, observed in radiographic images is an established indicator of cartilage degeneration [1]. Furthermore, the functional characteristics of the tissue such as stiffness [2,3], structural elasticity parameter – SEP [4] (a recently proposed parameter), fracture toughness and swelling resistance are calculated as functions of parameters such as strain and elastic strain energy, that are significantly dependent on material thickness. The importance of cartilage thickness to its characterization was earlier noted by Hayes et al. [5]. In fact, cartilage thickness and the difference in this parameter across a joint surface is a good indicator of cartilage condition and joint health, as can be seen in e.g. X-ray [6] and MRI [7] images.

MRI studies have shown that the thickness of cartilage varies across the joint [8], it is therefore essential to determine this parameter at each test site. This is even more so, if the measurement is to inform clinical decision in a precise manner. One method of assessing the functional characteristics of articular cartilage is indentation test, which provides the load–displacement characteristics of the tissue. Engineering parameters such as stiffness, recovery, and strain can then be evaluated from this relationship with the knowledge of the thickness of the tissue at the site of indentation [3,9–14]. However, measurement of this thickness in real-time during arthroscopic evaluation is not feasible with current effective and non-invasive methods such as MRI. It is argued herein that in order to achieve the goal of measuring cartilage thickness during arthroscopy of the joint, which has been elusive till now [3], the adaptation of a fast and non-destructive protocol, such as NIR, is required.

Several light propagated methods exist, and some have been applied to cartilage characterization and evaluation [15–17]; however, none of them possesses the depth penetrating property of near infrared (NIR) light, which has been shown to be approximately 8.5 mm in neonatal head [18]. To this end, a number of researchers have studied the potential of this method in evaluating low grade cartilage degradation [19,20], and distinguishing normal from enzymatically digested cartilage [21]. To the authors' knowledge, there is no published work on the use of NIR for quantifying physical properties, such as thickness, of the tissue.

Currently, non-mechanical systems such as near infrared [19,21,22], ultrasound [3] and magnetic resonance imaging, MRI,

* Corresponding author. Tel.: +61 731382158.
E-mail address: k.oloyede@qut.edu.au (A. Oloyede).

1350-4533/$ – see front matter © 2012 IPEM. Published by Elsevier Ltd. All rights reserved.
http://dx.doi.org/10.1016/j.medengphy.2012.04.003

[23] are being developed for characterizing this important tissue with the aim of potential clinical application and research. This paper does not intend to review these methods and hence the scope is limited to the consideration of the near infrared technique. The depth penetrating capacity of near infrared (approximately 8.5 mm in neonatal head [18]), provides a distinct advantage for probing full-thickness cartilage-on-bone (which is between 1 and 4 mm in humans) as demonstrated by the limited number of published studies [19–22,24]. Application of NIR probing for the properties of articular cartilage is fast developing, e.g. Spahn et al. [19,24] and Hoffman et al. [20] who proposed the parameter AR as an indicator of the water content of the tissue.

In a more recent study, Brown et al. [21] proposed the use of NIR for distinguishing normal from enzymatically digested cartilage based on the principal components and first derivative of their raw spectral data. While it is possible to recognize patterns in the spectra using principal components analysis, it is unlikely for variations in one spectral constituent (or wavelength) to vary in a manner that is exactly independent of any other due to the high collinearity of NIR spectral data. There is inevitably some correlation between the various constituents in a set of specimens; therefore any principal component will represent the sum of the effects of these correlated constituents [25]. Furthermore, it is not exactly clear which structural or functional properties of the tissue are represented by the principal component, and how they could be used in research and clinical evaluation.

Various methods are available for measuring the thickness of articular cartilage. These include in vitro (and invasive) methods such as anatomical sectioning or punch-probes [26–28], needle probe, optical [10,12,29], and stereophotogrammetry [30]. These methods are effective for laboratory and in vitro purposes, however, they are either destructive or cannot be easily adapted for real-time applications, e.g. during surgery. A-mode pulse-echo ultrasound [29,31,32] is a notable non-destructive technique that is often used for the determination cartilage thickness; however its accuracy is limited because of the difficulty involved in determining precisely the speed of the ultrasound wave in cartilage. This varies according to the pathological condition of the tissue [3]. Another method that has been used for approximating the thickness is magnetic resonance imaging (MRI). It is also non-destructive and can be non-invasive [33–35]. Thickness values obtained using this method has been shown to correlate with those of anatomical sections [36]. Nevertheless, the application of this method in real-time during clinical/surgical procedures such as arthroscopy is impractical and can also be costly.

This study considers the question of whether or not near infrared spectroscopy can provide a framework for the non-destructive determination of cartilage thickness that can contribute to an innovation for clinical practice and surgery. To address this question, the thickness of visually intact cartilage samples were obtained using an electronic vernier caliper and the needle probe mechanized method [29]. The relationship between each sample's thickness and its near infrared absorption spectrum were evaluated using single *y*-variable partial least squares regression (PLS1) [37]. The relationships obtained were then optimized for accurate prediction of unknown sample thickness values using a robust PLSR algorithm – bagging-PLS [38,39].

2. Materials and methods

2.1. Cartilage sample preparation

Visually normal and intact bovine patellae ($N = 15$), harvested from 2 to 3 year old prime oxen within 24 h of slaughter, were used in this study. The samples were wrapped in 0.15 M saline soaked towels and stored at −20 °C until required for testing. Prior to NIR spectroscopy, the intact patellae were thawed in 0.15 M saline at room temperature for about 4 h, then cartilage-on-bone blocks ($n = 97$, $l \times b \times h = 7 \times 7 \times 5$ mm) were cut with an arc saw while the patella samples were held tight with a vice. This was performed in a manner that only the bone was in contact with the vice during the cutting operation so that there is no damage to the cartilage. All tests were conducted with the specimens fully submerged in 0.15 M saline.

Subsequent to NIR spectroscopy, the thickness of each specimen was obtained using two different protocols from the literature, namely manual (using the vernier caliper) and needle probe [29] methods.

2.2. Near infrared spectroscopy – instrumentation and data acquisition

Diffuse reflectance near infrared spectroscopy was performed using a Bruker MPA™ (Multi-Purpose Analyser) FT-NIR (Fourier Transform Near Infrared) spectrometer (Bruker Optics, Germany). The source lamp emits light of wavelength 800–2500 nm (12,500–4000 cm^{-1} wavenumber); which covers the full range of the near infrared region of the electromagnetic spectrum. NIR spectral data were acquired in diffuse reflectance mode using a fibre optic probe consisting of 100 optical fibre bundles (ø = 600 μm per strand, 50 fibres per set; one set for transmitting the NIR light and the other for receiving the reflected light from the specimen. The spectrometer was connected to a personal computer running the Bruker OPUS 6.5 software, through which the equipment was triggered for sample measurement and for spectral data acquisition.

From preliminary experiments to determine non-tissue factors that could affect the near infrared signal, it was observed that offset from the tissue surface and vibration of the probe during scanning significantly affected the repeatability of the output spectra. To address and minimize the effects of these factors, an experimental rig was constructed to keep the probe stable during scanning. The rig consists of a steel plate, for holding the specimen, and placed in position on an adjustable *x*–*y* base plate. This plate sits directly under a *z*-axis guide which holds the fibre probe in position. Prior to sample scanning, a reference spectrum was taken from a spectralon reflectance standard – *SRS-99* (Labsphere Inc., North Sutton, USA), embedded in the spectrometer. The probe was lowered (until it touches the specimen's surface) and firmly locked in position, ready for scanning. Spectral data was obtained over the full range of the NIR spectrum at 16 cm^{-1} resolution, with each spectrum averaged over 64 scans. The NIR absorbance spectrum (plot of $\log(1/R)$ against wavenumber, where R = reflectance) for each specimen was obtained with an approximate scan time of 20 s.

2.3. Manual measurement

Following NIR spectroscopy, each osteochondral block specimen was held under a microscope (for magnification) with one of its sides facing upward. A high precision digital vernier caliper was then used to obtain the thickness of the uncalcified cartilage. This procedure was repeated for all four sides of each specimen and the mean of the measurement taken as the representative thickness of the specimen.

2.4. Needle probe measurement

After manual measurement of cartilage thickness, the specimens were mounted for needle probe thickness measurement. Each cartilage-on-bone specimen was set in dental acrylic cast

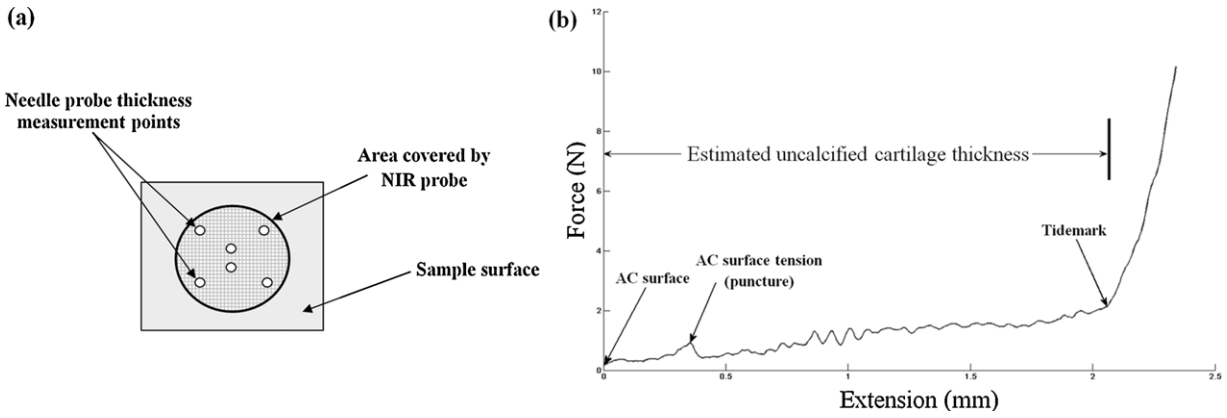

Fig. 1. (a) View of sample surface showing the area covered by the NIR probe during scanning and the points where the needle probe thickness measurement were obtained. (b) Needle probe Force–Extension curve showing the estimated cartilage thickness.

(Palapress Vario®), with the subchondral bone immersed in the acrylic mixture and the cartilage surface slightly above and parallel to the cast surface, and left to cure. This ensured that the specimen was held fixed and perpendicular to the needle probe during indentation.

The samples were then mounted on a high resolution mechanical testing machine, Hounsfield® Test Equipment (HTE). An indenter carrying a needle probe was attached to the load cell of the test device, with the speed of indentation set to 10 mm/min in accordance with the method of Jurvelin et al. [29]. With the sample surface perpendicular to the needle probe, the probe was gently lowered in micron steps until it just touches (but not indenting) the tissue surface. The thickness of the cartilage sample was measured at six different points under the region where the NIR spectrum was obtained (Fig. 1(a)) by using the load cell to sense the instant when the needle touches the articular surface and when it contacts the calcified zone.

The Force–Extension curve was obtained and displayed on the PC. The profile of the needle as it travels from the tissue surface, through the uncalcified cartilage, to the tidemark is presented in Fig. 1(b). The thickness of the uncalcified cartilage is obtained as the extension from the surface to the tidemark; which is characterized by a change in slope of the curve (Fig. 1(b)) due to the difference in material properties of the uncalcified and calcified cartilage or tidemark.

3. Results

3.1. Near infrared spectroscopy

Variations in the near infrared absorption spectra with sample thickness can be observed in the baseline corrected spectral plots of Fig. 2 The data set were collected and randomly split into two subsets; the calibration set for training, and the test/validation set for testing the developed multivariate (PLS) model. Four-fifths of the data ($n = 79$) were used for training, i.e. to fit the models, and the remaining fifth ($n = 18$) for testing. The test data set were set aside independent of the training procedure. It was also ensured that both data sets spanned the full distribution of the overall data set.

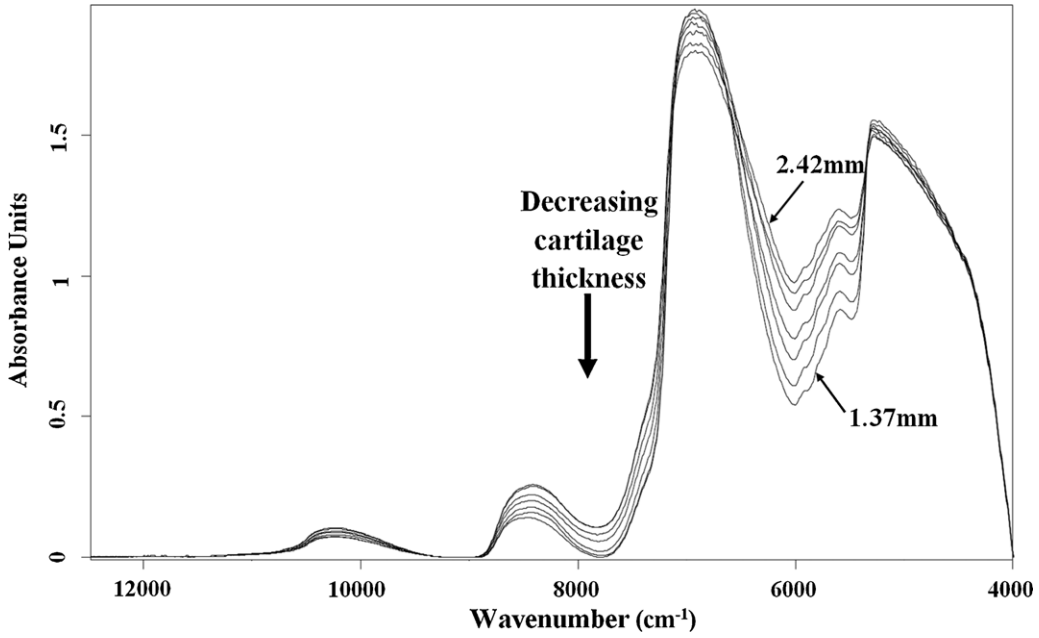

Fig. 2. Baseline corrected near infrared absorption spectra showing variation with cartilage thickness.

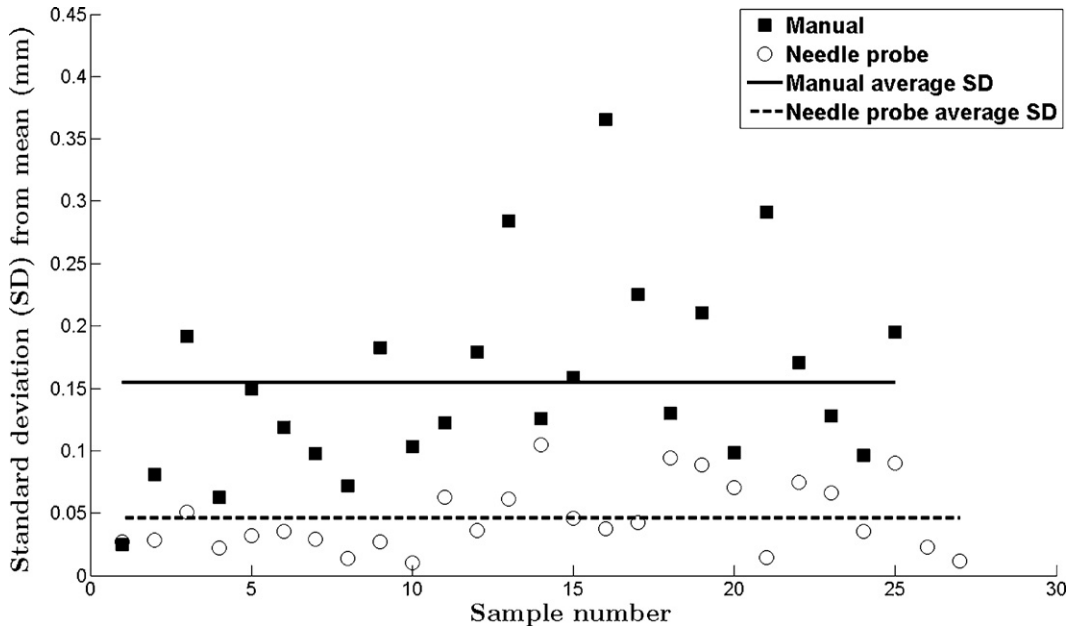

Fig. 3. Scatter plot showing the deviation of each sample mean from the individual thickness measurements for manual and needle probe (NP) thickness.

3.2. Mechanical measurement of cartilage thickness

The manually measured thickness values from each side of a sample were averaged and used as the representative thickness for that sample. The final thickness value of each sample obtained using the needle probe method was evaluated as the average of the six measurements taken at points within the regions under which the NIR spectrum was obtained (Fig. 1(a)). The thickness for all samples tested ranges from 1.20 to 2.42 mm.

3.3. Selection of correlated cartilage thickness (response variable)

The data of manual thickness values obtained from all four sides of the samples, and those obtained from six needle probe points under the area where NIR absorbance measurements were taken were compared using a two-tailed, paired Student *t*-test. The results reveal that the average values for the manual and needle probe measurements (1.75 ± 0.15 mm) and (1.77 ± 0.05 mm) respectively, were comparable ($p = 0.63$).

It should be noted that on closer inspection of the standard deviation of the manually measured thickness, a significantly higher deviation or scatter ($p < 0.0001$) was revealed, in comparison to the needle probe measured thickness, as presented in Fig. 3. The average deviation from the mean for manual method is 0.1546 mm, and that for needle probe technique is 0.0457 mm. For this reason, the more stable needle probe thickness values were used as the response variables in the statistical correlation that was performed in this study.

4. Data analysis

4.1. Spectral preprocessing

Partial least squares (PLS) regression method, used to find fundamental relationships between predictor and response variables, was employed as the multivariate statistical technique in this study. Being a linear regression technique, PLS may not always model raw spectral data efficiently as some of the relationships between the spectra and cartilage properties may be non-linear and possibly multicollinear. As a result, non-linearities, such as those resulting from light scattering variations in reflectance spectroscopy [40], may be linearized using transformations, preprocessing and pretreatment algorithms, or may be avoided altogether using wavelength selection techniques [39]. In this study, both approaches were adapted to optimize the relationship between the predictor and response variables. Spectral analysis and preprocessing were performed using ParLeS: software for chemometrics and spectroscopy [41]. Prior to analysis, each specimen's average needle probe thickness (response) and corresponding NIR spectral data (predictors) were collected and formatted as specified in the software suite [41].

To correct for light scatter and other non-linearities, spectral preprocessing, denoising and pretreatment techniques were implemented on the raw NIR spectral data. The preprocessing techniques investigated include multiplicative scatter correction (MSC), standard normal variate (SNV), wavelet detrending, and a combination of SNV with wavelet detrending. Following preliminary analysis using a single *y*-variable partial least squares (PLS1) regression method on the calibration data set, SNV with wavelet detrending was found to be the most efficient for preprocessing the predictor variables. A 2-level Wavelet filter was employed for denoising the data and mean centring was used for pretreatment (Fig. 4).

Using wavelength selection technique, the preprocessed spectral data were divided into five distinct regions of interest (Fig. 4), with each region (and combination of regions) used in the multivariate calibration protocol for correlation with cartilage thickness.

4.2. PLS1 calibration, validation, and prediction

The preprocessed data for each region (specified in Fig. 4) were separately calibrated (modelled) for prediction of articular cartilage thickness. A combination of regions: $A_6 = A_4 + A_5$, $A_7 = A_3 + A_4$, and $A_8 = A_3 + A_4 + A_5$, were also considered for multivariate calibration. Leave-one-out (LOO) cross-validation was used to estimate prediction error and coefficient of determination for model selection, and a maximum of 10 PLS components were tested. To avoid under- or over-fitting, while accounting for as much variation in the

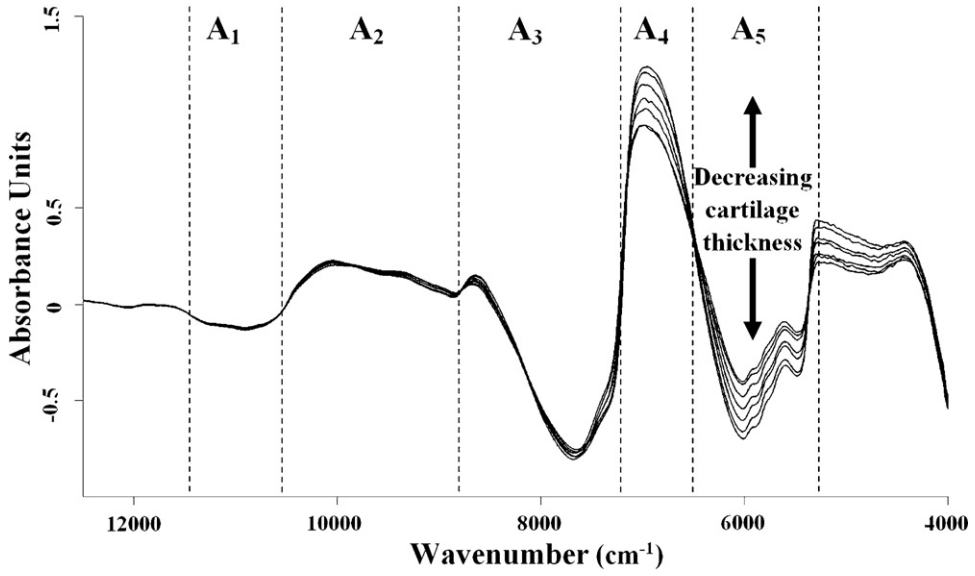

Fig. 4. Near infrared absorption spectral variation with cartilage thickness following (SNV with wavelet detrending, wavelet filtering, and mean centring) preprocessing, and showing the selected regions for correlation with cartilage thickness.

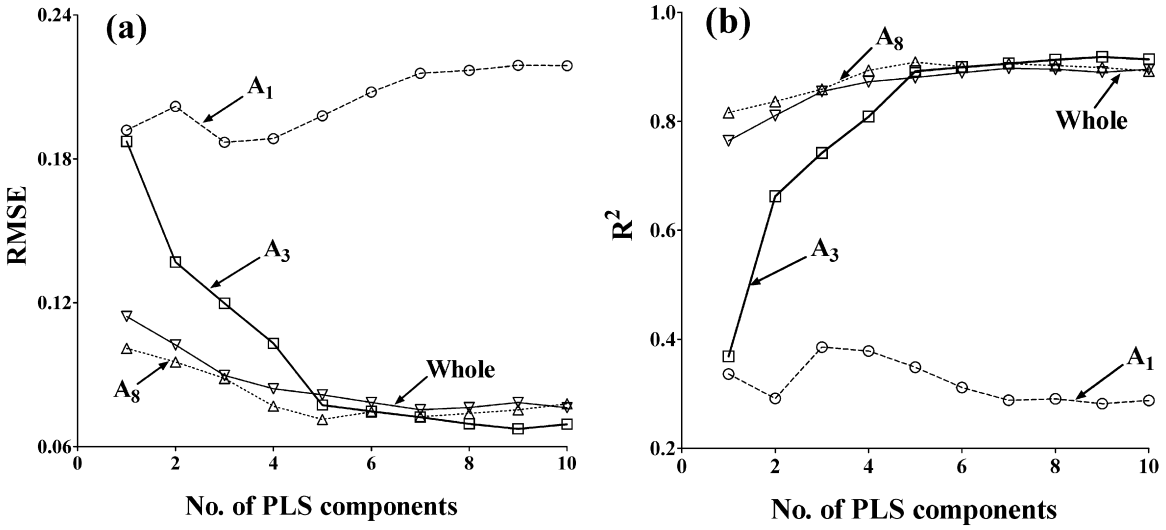

Fig. 5. PLS assessment statistics showing variation of (a) RMSE, and (b) R^2, with the number of PLS components for four of the spectral regions tested.

predictor variables, selection of the optimal model was based on the minimum root mean square error (*RMSE*) and maximum coefficient of determination (shown as X_{val} R^2 in Table 1) of cross-validation, indicating the "goodness of fit" of the selected model (Fig. 5(a) and (b)). After cross-validation and optimal model selection, assessment of the model's efficiency in predicting new samples, independent of the calibration set, was validated using the test data set and assessed based on their prediction R^2 (shown as Pred R^2 Table 1).

From the assessment statistics of Table 1, the models developed based on regions A_3 and A_8 indicate an improvement in calibration and prediction accuracy in comparison to the model developed with the whole spectral range. Region A_1 gave the poorest correlation with the tissue thickness. The PLS1 calibration and validation plots for the selected model are presented in Fig. 6(a)–(d). These plots confirm the linear relationship between the NIR spectral data and the tissue thickness.

Table 1
PLSR assessment statistics of cartilage thickness to NIR correlation based on distinct regions of the spectrum, X_{val} = cross-validation, Pred = prediction.

Regions	N_{calib} = 79; N_{test} = 18; 10 components tested Preprocessing: SNV + Wavelet filter + mean centring				
	Range (cm^{-1})	Comp	X_{val} R^2 (%)	RMSEP	Pred R^2 (%)
A_1	11,500–10,500	3	39.4	0.187	67.7
A_2	10,500–8850	5	37.5	0.19	53.1
A_3 [a]	8850–7200	6	91.9	0.067	90.7
A_4	7200–6500	4	79.3	0.119	73.7
A_5	6500–5350	6	90.6	0.073	88.8
A_6	7200–5350	7	88.8	0.079	88.4
A_7	8850–6500	8	88.3	0.081	84.1
A_8 [a]	8850–5350	5	90.8	0.071	91.5
Whole	12,500–4000	7	89.9	0.075	91.4

[a] Regions with improvement in calibration compared to the whole spectrum.

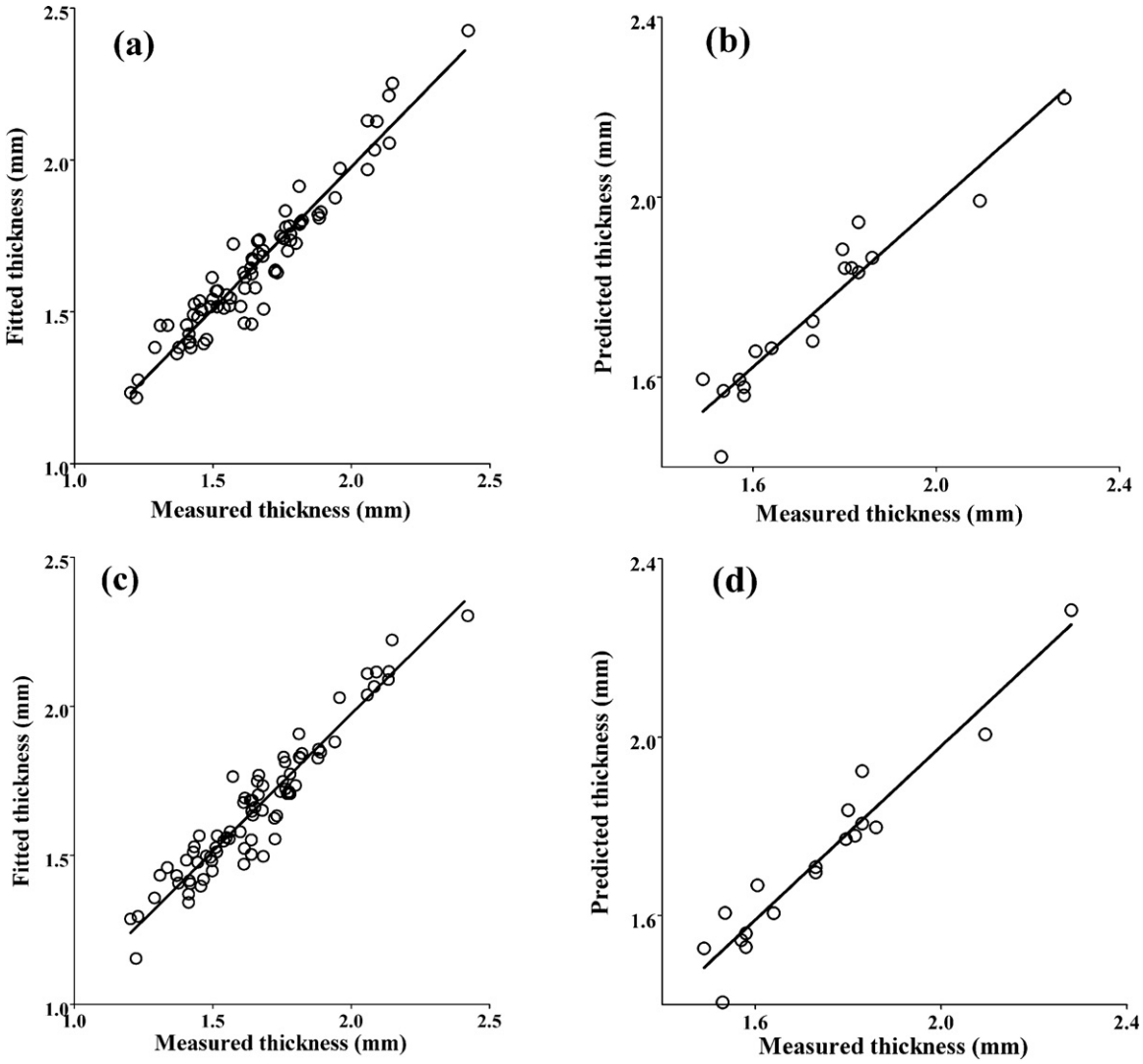

Fig. 6. Correlation plot showing (a) calibration (R^2 = 91.9%, p < 0.0001) and (b) prediction (R^2 = 90.7%, p < 0.0001) relationship for region A_3; (c) calibration (R^2 = 90.8%, p < 0.0001) and (b) prediction (R^2 = 91.5%, p < 0.0001) relationship for region A_8.

Table 2
Assessment statistics showing the performance of conventional PLS1 and bagging-PLS in the prediction of cartilage thickness based on regions A_3 and A_8.

Regions	PLS1		Bagging PLS	
	R^2 (%) p < 0.0001	RMSEP	R^2 (%) p < 0.0001	RMSEP
A_3	90.7	0.067	92.3	0.055
A_8	91.5	0.071	93.1	0.056

4.3. Bagging PLS regression

Bootstrap aggregation- or bagging-PLS, a robust variant of PLS, was investigated for calibrating the relationship between the regions A_3 and A_8 of cartilage NIR spectra and its thickness. This technique has been reported to yield improvements in accuracy of regression models, especially when alteration of the training data set can cause significant changes in the outcome of the modelling procedure [38]. 30 bootstraps (i.e. B = 30) was used here, with the selection of B based on bootstraps replicates for regression reported by Breimen [38] who suggested using approximately 25 bootstraps.

The statistics of Table 2 present a comparison of assessment results using traditional PLS1 versus bagging-PLSR in the model development and validation process. Decrease in the *RMSE* and increase in the R^2 for both regions were observed using the bootstrapping protocol with PLS.

5. Discussion

In the present study, we have established that, using multivariate analysis, it is possible to non-destructively obtain articular cartilage thickness using diffuse reflectance near infrared spectroscopy. Correlations between the spectra and the tissue thickness were investigated using distinct regions and whole spectral range. Increase in calibration and prediction accuracy were observed with models based on regions A_3 and A_8 over that based on the whole spectrum (Table 1). It should be noted that only bovine cartilage has been studied in this research and a recalibration would be required for the human tissue; it is however not expected that a large discrepancy that would distort the philosophical underpinning of the work would result from such analysis. The thickness measurement accuracy reported in this study using the robust bagging-PLS, with a 5.6% error margin, i.e. 0.098 mm (Table 2), is comparable with well established non-destructive methods in the literature such as MRI [7,8]. However, it should be noted that both

methods may not be directly comparable since they are subject to reference methods which may differ.

The errors in the developed models are likely to be those propagated from the reference method to the calibration, via the response variables, because the prediction capacity of any PLS model is dependent on the accuracy and stability of the response variables. The needle probe method provides reliable thickness data for use as response variables because it gives a more accurate measure of the tissue's thickness compared to methods such as A-mode ultrasound [3], and a more stable estimation in comparison to the manual method. However, it results in destruction of the tissue structure at the site of measurement, restricting further use of the specimen and making it only suitable if cartilage thickness is not necessary before mechanical test. Even so, these drawbacks are not demerits in this study as the aim is to develop a calibration model that is capable of relating cartilage thickness to its NIR spectra with as little error as possible. Other possible sources of error include light scatter, instrument based non-linearities [40] and environmental conditions which have been controlled and compensated for using spectral pretreatment and judicious experimental setup.

With the manual method, rupturing of the fibrous collagenous structure of articular cartilage during sample preparation is likely to produce extra swelling of the tissue when immersed in aqueous solution and cause an artefactual increase of the measured thickness [25]. This is arguably the reason for the significantly high standard deviation of thickness values measured using this method. Hence, because of this high SD, which we believe reflects the inherent error in the method the manual thickness was eliminated. Furthermore, the manual method was only able to measure at regions peripheral to the probed regions.

The scattering of NIR light by mammalian tissue has a strong forward component; however, for optically dense samples such as articular cartilage, the diffuse reflection (or backscattering) mode is often utilized [18]. While this is advantageous for probing deep within the cartilage matrix, it is necessary to deal with the undesirable effects of light scatter and noise associated with this method. Data preprocessing and pretreatment algorithms were implemented prior to analysis (Fig. 4) in order to address these inevitable effects, and increase the accuracy and robustness of the calibration models.

Beside the improvement in accuracy, correlations based on distinct regions of the spectrum provide an insight into the specific component(s) of the matrix used as an indicator or measure of the cartilage thickness. The region A_3 is characterized by second overtone CH vibrations and is likely to be indicative of the matrix collagen meshwork, while A_8 encompasses regions characterized by first and second overtone CH and OH peaks and is arguably representative of the major matrix components; collagen, proteoglycan and water. Cartilage thickness can thus be argued to be linearly correlated with the total near infrared absorption (or diffuse reflection) encountered in the tissue matrix as the light travels from the surface, through the matrix material, to the optically dense subchondral bone. Hence, the cartilage thickness can be conceptualized as the effective pathlength encountered by the light as it travels through the tissue to the optically opaque underlying bone.

Analysis based on regions A_3 and A_8 does not only yield more accurate and robust calibration models, but also present a computationally faster option to using the whole spectrum. They require significantly less time for analysis (3–6 times less for cross-validation) relative to the whole spectrum (Table 3). A considerable decrease in the total time for analysis based on regions A_1 and A_4 would be a reasonable expectation due to the relatively small size of X (predictor variables). However, a dramatic increase in total analysis time, particularly during principal component (PC) decomposition, can be observed (Table 3). This may be attributed to the weak (or lack of useful) information and higher noise levels in these regions, making it difficult for the PLS algorithm to generate/obtain linear transformations (latent variables) of the original data in such a way that the information is maximally preserved (in minimum mean squared error sense). This is also due, in part, to the overwhelming NIR light absorption characterized by the water peak in region A_4.

Table 3
PLS performance and running times for the investigated regions based on PCA and PLS cross-validation computations using a 3.33 GHz core™ 2 duo processor with 3.46 GB RAM in a Windows XP environment.

Regions	No. of components tested = 10				
	Range (cm^{-1})	Size of X	Running times (s)		
			PCA	PLSR X_{val}	Total
A_1	11,500–10,500	131	103.9	1	104.9
A_2	10,500–8850	215	75.7	1.5	76.2
A_3 [a]	8850–7200	215	30.2	1.7	31.9
A_4	7200–6500	92	106.7	0.8	107.5
A_5	6500–5350	150	54.1	1	55.1
A_6	7200–5350	241	69.5	1.7	71.2
A_7	8850–6500	306	55.8	2.1	57.9
A_8 [a]	8850–5350	455	33.4	2.7	36.1
Whole	12,500–4000	1102	40.9	7.1	48

[a] Regions with improvement in running times compared to the whole spectrum.

The technique proposed in this study is similar to an optical method proposed by Johansson et al. [17] for assessing tissue qualities. Their method employs light in the spectral range of 25,000–12,500 cm^{-1}, and uses the amount of detected photon from the tissue to determine its matrix thickness. This method is only applicable to tissues that are less than 1.2 mm in thickness and therefore much less than the thickness of the human cartilage which is approximately 4 mm. Consequently, the protocol reported in this paper constitutes a significant step in the development of a method for measuring the thickness of human cartilage without a mechanical aid.

The correlation analysis using the robust bagging-PLSR technique on specific regions (A_3 and A_8) of the spectrum yielded improvement in accuracy (Table 2) making this method adaptable for clinical/surgical determination of cartilage thickness. Furthermore, computational efficiency of this method and the proposed regions is a favourable outcome for facilitating fast, real-time non-destructive determination of the tissue property for both research and clinical use. Of importance is that the method is arguably capable of delivering significant benefits to the arthroscopic evaluation and treatment of joint ailment involving degenerated articular cartilage.

In comparison with methods such as MRI, the thickness determined by the method proposed cannot provide diagnosis in its innate form. It has to be used to calculate parameters such as stiffness that can be used for categorizing the condition of cartilage. Furthermore, it must be applied in contact with the tissue, which again provides a contrast to imaging and diagnostic procedures like MRI and X-ray radiography. In addition, its accuracy depends on the reliability of the statistical predictive model applied, and the reference data used. This requirement was addressed in this research by obtaining the thickness values via two methods, namely manual and needle probe methods, before statistically selecting the data from the needle probe method to be used as reference in the development of the calibration model.

In summary, a translation of the method to the clinical environment is plausible, where deformation parameters are calculated and used to distinguish cartilage in one

region from the other via the following sequence of analyses.

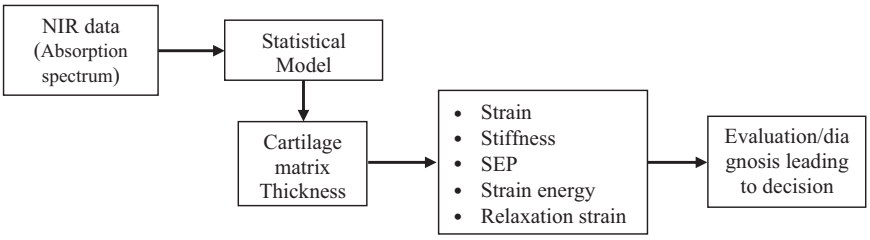

Conflict of interest

All the authors declare that there is no conflict of interest.

References

[1] Kellgren JH, Lawrence JS. Radiological assessment of osteo-arthrosis. Ann Rheum Dis 1957;16(4):494–502.
[2] Lane JM, Chisena E, Black J. Experimental knee instability: early mechanical property changes in articular cartilage in a rabbit model. Clin Orthop Relat Res 1979;140:262–5.
[3] Suh J-KF, Youn I, Fu FU. An in situ calibration of an ultrasound transducer: a potential application for an ultrasonic indentation test of articular cartilage. J Biomech 2001;34:1347–53.
[4] Brown CP, Crawford RW, Oloyede A. An alternative mechanical parameter for assessing the viability of articular cartilage. J Eng Med 2009;223:53–62.
[5] Hayes WC, Keer LM, Herrmann G, Mockros LF. A mathematical analysis for indentation tests of articular cartilage. J Biomech 1972;5:541–51.
[6] Buckland-Wright JC, Macfarlane DG, Lynch JA, Jasani MK, Bradshaw CR. Joint space width measures cartilage thickness in osteoarthrosis of the knee: high resolution plain film and double contrast macroradiographic investigation. Ann Rheum Dis 1995;54:263–8.
[7] Cohen ZA, McCarthy DM, Kwak SD, Legrand P, Fogarasi F, Ciaccio EJ, Ateshian GA. Knee cartilage topography, thickness, and contact areas from MRI: invitro calibration and in vivo measurements. Osteoarthr Cartilage 1999;7:95–109.
[8] Li G, Park SE, DeFrate LE, Schutzer ME, Ji L, Gill TJ, Rubash HE. The cartilage thickness distribution in the tibiofemoral joint and its correlation with cartilage-to-cartilage contact. Clin Biomech 2005;20:736–44.
[9] DiSilvestro MR, Suh JKF. A cross-validation of the biphasic poroviscoelastic model of articular cartilage in unconfined compression, indentation, and confined compression. J Biomech 2001;34:519–25.
[10] Hoch DH, Grodzinsky AJ, Koob TJ, Albert ML, Eyre DR. Early changes in material properties of rabbit articular cartilage after meniscectomy. J Orthop Res 1983;1:4–12.
[11] Lyyra T, Jurvelin J, Pitkanen U, Vaatainen U, Kiviranta I. Indentation instrument for the measurement of cartilage stiffness under arthroscopic control. Med Eng Phys 1995;17:395–9.
[12] Mow VC, Gibbs MC, Lai WM, Zhu WB, Athanasiou KA. Biphasic indentation of articular cartilage: II. A numerical algorithm and an experimental study. J Biomech 1989;22:853–61.
[13] Newberry WN, Mackenzie CD, Haut RC. Blunt impact causes changes in bone and cartilage in a regularly exercised animal model. J Orthop Res 1998;16:348–54.
[14] Niederauer MQ, Cristante S, Niederauer GM, Wilkes RP, Singh SM, Messina DF, Walter MA, Boyan BD, DeLee JC, Niederauer G. A novel instrument for quantitatively measuring the stiffness of articular cartilage. In: Transactions of the 44th orthopedic research society. 1998.
[15] Camacho NP, West P, Torzilli PA, Mendelsohn R. FTIR microscopic imaging of collagen and proteoglycan in bovine cartilage. Biopolymers 2001;62:1–8.
[16] Boskey A, Camacho NP. FT-IR imaging of native and tissue-engineered bone and cartilage. Biomaterials 2007;28:2465–78.
[17] Johansson A, Sundqvist T, Oberg A. Arrangement and method for assessing tissue qualities. United States Patent Office, app. no. 10/587,490; 2007.
[18] Faris F, Thorniley M, Wickramasinghe Y, Houston R, Rolfe P, Livera N, Spencer A. Noninvasive invivo near-infrared optical measurement of the penetration depth in the neonatal head. Clin Phys Physiol Measur 1991;12(4):353–8.
[19] Spahn G, Plettenberg H, Nagel H, Karl E, Klinger HM, Muckley T, Gunther M, Hofman GO, Mollenhauer JA. Evaluation of cartilage defect with near infrared spectroscopy (NIR): an ex vivo study. Med Eng Phys 2007;30:285–92.
[20] Hofman GO, Marticke J, Grossstuck R, Hoffman M, Lange M, Plettenberg HK, Braunschweig R, Schilling O, Kaden I, Spahn G. Detection and evaluation of initial cartilage pathology in man: a comparison between MRT, arthroscopy and near-infrared spectroscopy (NIR) in their relation to initial knee pain. Pathophysiology 2010;17(1):1–8.
[21] Brown CP, Bowden JC, Rintoul L, Meder R, Oloyede A, Crawford R. Diffuse reflectance near infrared spectroscopy can distinguish normal from enzymatically digested cartilage. Phys Med Biol 2009;54:5579–94.
[22] Afara I, Sahama T, Oloyede A. Near infrared for non-destructive testing of articular cartilage. In: Nondestructive testing of materials and structures. Istanbul, Turkey: Springer; 2011.
[23] Tiderius CJ, Jessel R, Kim Y-J, Burstein D. Hip dGEMRIC in asymptomatic volunteers and patients with early osteoarthritis: the influence of timing after contrast injection. Magn Reson Med 2007;57:803–5.
[24] Spahn G, Plettenberg H, Kahl E, Klinger HM, Muckley T, Hofman GO. Near-infrared (NIR) spectroscopy. A new method for arthroscopic evaluation of low grade degenerated cartilage lesions. Results of a pilot study. BMC Musculoskelet Disord 2007;8:47.
[25] Howard M. Qualitative discriminant analysis. In: Burns AD, Ciurczak EW, editors. Handbook of near infrared analysis. New York: Marcel Dekker, Inc.; 2001.
[26] Eckstein F, Muller-Gerbl M, Putz R. Distribution of subchondral bone density and cartilage thickness in the human patella. J Anat 1992;180:425–33.
[27] Meachim G, Bentley G, Baker R. Effect of age on thickness of adult patellar articular cartilage. Ann Rheum Dis 1977;36:563–8.
[28] Muller-Gerbl M, Schulte E, Putz R. The thickness of the calcified layer of articular cartilage: a function of the load supported? J Anat 1987;154:103–11.
[29] Jurvelin JS, Rasanen T, Kolmonen P, Lyyra T. Comparison of optical, needle probe and ultrasonic techniques for the measurement of articular cartilage thickness. J Biomech 1995;28:231–5.
[30] Ateshian GA, Soslowsky LJ, Mow VC. Quantitation of articular surface topography and cartilage thickness in knee joints using stereophotogrammetry. J Biomech 1991;24:761–76.
[31] Modest VE, Murphy MC, Mann RW. Optical verification of a technique for in situ ultrasonic measurement of articular cartilage thickness. J Biomech 1989;22:171–6.
[32] Rushfeldt PD, Mann RW, Harris WH. Improved techniques for measuring in vitro the geometry and pressure distribution in the human acetabulum – I. Ultrasonic measurement of acetabular surfaces; sphericity and cartilage thickness. J Biomech 1981;14:256–60.
[33] Eckstein F, Gavazzeni A, Sittek H, Hauhner M, Losch A, Milz S, Englmeier K-H, Schulte E, Putz R, Reiser M. Determination of knee joint cartilage thickness using three-dimensional magnetic resonance chondro-crassometry (3D MR-CCM). Magn Reson Med 1996;36:256–65.
[34] Muensterer OJ, Eckstein F, Hahn D, Putz R. Computer-aided three dimensional assessment of knee joint cartilage with magnetic resonance imaging. Clin Biomech 1996;11:260–6.
[35] Andreisek G, White LM, Sussman MS, Kunz M, Hurtig M, Weller I, Essue J, Marks P, Eckstein F. Quantitative MR imaging evaluation of the cartilage thickness and subchondral bone area in patients with ACL-reconstructions 7 years after surgery. Osteoarthr Cartilage 2009;17:871–8.
[36] Eckstein F, Sittek H, Milz S, Schulte E, Kiefer R, Reiser M, Putz R. The potential of magnetic resonance imaging (MRI) in quantifying the regional distribution of articular cartilage thickness—a methodological study. Clin Biomech 1995;10:434–40.
[37] Bjørsvik H-R, Martens H. Data analysis: calibration of NIR instruments by PLS regression. In: Burns AD, Ciurczak EW, editors. Handbook of near infrared analysis. 2nd edition. New York: Marcel Dekker, Inc.; 2001.
[38] Breimen L. Bagging predictors. Mach Learn 1996;24:123.
[39] Viscarra Rossel RA. Robust modelling of soil diffuse reflectance spectra by "bagging-partial least squares regression". J Near Infrared Spectrosc 2007;15:39–47.
[40] Geladi P, MacDougall D, Martens H. Linearization and scatter-correction for near infrared reflectance spectra of meat. Appl Spectrosc 1985;39(3):491–500.
[41] Viscarra Rossel RA. ParLeS: software for chemometric analysis of spectroscopic data. Chemometr Intell Lab Syst 2008;90:72–83.